Catalysis Science & Technology

PAPER

View Article Online
View Journal | View Issue

Cite this: *Catal. Sci. Technol.*, 2014, 4, 997

# A polyhedral oligomeric silsesquioxane (POSS)-bridged oxo-molybdenum Schiff base complex with enhanced heterogeneous catalytic activity in epoxidation

Yan Leng,* Jian Liu, Chenjun Zhang and Pingping Jiang

Received 4th December 2013,
Accepted 4th January 2014

DOI: 10.1039/c3cy01014g

www.rsc.org/catalysis

We have generated a new heterogeneous catalyst by bridging an oxo-molybdenum Schiff base on a polyhedral oligomeric silsesquioxane (POSS) *via* covalent attachment. The resulting POSS-bridged oxo-molybdenum Schiff base complex catalyst was fully characterized by $^1$H NMR, XRD, FT-IR, SEM, TGA, and contact angle analysis, and its catalytic potential was studied for the epoxidation of alkenes using aqueous *tert*-butyl hydroperoxide (TBHP) as the oxidant. The catalyst was found to be highly efficient and showed higher catalytic reactivity than the corresponding homogeneous analogues with added benefits of facile recovery and recycling of the heterogeneous catalyst. The POSS-bridged oxo-molybdenum Schiff base complex was successfully reused for four runs without significant loss in activity. The unique three dimensional network catalyst structure and the hydrophobic properties of the POSS units in the catalyst are revealed to be responsible for the catalyst's excellent performance in epoxidation reactions.

## 1. Introduction

Polyhedral oligomeric silsesquioxanes (POSS), an intriguing class of organic–inorganic hybrid materials, possess a cubic structure represented by the formula $R_8Si_8O_{12}$, in which the central hydrophobic inorganic core ($Si_8O_{12}$) is surrounded by organic moieties at the eight vertices.[1,2] Their unique star-shaped nanostructures and chemical properties, such as facile chemical modification, good pH tolerance, and high temperature and oxidation resistance properties, make POSS an ideal building block for constructing multi-functional materials by introducing functional groups and elements.[3–6] Despite the versatile applications of POSS in many materials, such as dental restorative materials, drug delivery agents, liquid crystal materials, and light-emitting materials among others,[7–11] POSS have not been extensively explored for catalytic applications facilitating useful chemical transformations even though this area has immense potential. Recently, only a few studies have focused on investigation of POSS-based heterogeneous catalysts. For example, Wada[12] described the preparation of silica-supported Ti oxide catalysts using Ti-containing POSS as precursors, with the resultant product showing high catalytic activity and stability in epoxidation of cyclooctene. Grela[13] reported a POSS-tagged Grubbs–Hoveyda-type olefin catalyst, which can be recovered using nanofiltration techniques and can be reused. These reports have shown that POSS can function as carriers or activity promoters for developing highly efficient heterogeneous catalytic systems.

The transformation of alkenes to corresponding epoxides is both an important industrial technology and a useful synthetic method for a wide range of products including pharmaceuticals and agrochemicals.[14–17] Metal Schiff base complexes are known to be good homogeneous epoxidation catalysts due to their high activity and selectivity.[18–20] However, problems in catalyst separation and recyclability should be addressed for these homogeneous catalysts. To this end, several strategies involving immobilization of the active catalytic moiety, *viz.* to zeolites, polymers, silica, layered double hydroxides, and amine-functionalized hexagonal mesoporous hydroxides, have been reported.[21–26] Though good activity was achieved in those cases, most of them still bear some drawbacks like slow reaction speed, low catalyst loading, leaching of active species, or limited accessibility to the reactants. A new strategy for catalyst preparation to overcome the above problems is therefore highly desirable.

In this paper, we utilize aminopropyl-POSS reagent as the monomer for the preparation of a POSS-bridged oxo-molybdenum Schiff base complex *via* covalent attachment with an oxo-molybdenum Schiff base and then use it as the catalyst for epoxidation reactions. It supplies a unique three dimensional network structure and isolates each substituted

---

*The Key Laboratory of Food Colloids and Biotechnology, Ministry of Education, School of Chemical and Material Engineering, Jiangnan University, Wuxi 214122, China. E-mail: lengyan1114@126.com; Fax: +86 510 85917763; Tel: +86-510-85917090*

oxo-molybdenum Schiff base group on the vertices of POSS, which would provide high stiffness and stability beneficial for the homogeneous distribution of the active centers. Moreover, hydrophobicity of the POSS core surrounded by the oxo-molybdenum Schiff base would facilitate the access of reactants to the reactive oxo-molybdenum centers. To the best of our knowledge, there is no report on the use of POSS as monomers for the immobilization of an organometallic complex in order to facilitate its efficiency and recycling during an organic transformation. Catalytic tests for the epoxidation of various alkenes using aqueous *tert*-butyl hydroperoxide (TBHP) as the oxidant, along with comparisons to its homogeneous analogues, well demonstrate that this newly designed solid complex is a highly active and selective, reusable, and non-leaching catalyst for the epoxidation reactions.

## 2. Experimental section

### 2.1 Reagents and analyses

All chemicals were of analytical grade and used as received. FT-IR spectra were recorded on a Nicolet 360 FT-IR instrument (KBr discs) in the 4000–400 cm$^{-1}$ region. $^1$H-NMR spectra were measured on a Bruker DPX 300 spectrometer at ambient temperature in $D_2O$ or $CDCl_3$ using TMS as the internal reference. TG analysis was carried out using a STA409 instrument in dry air at a heating rate of 10 °C min$^{-1}$. SEM was performed on a HITACHI S-4800 field-emission scanning electron microscope. XRD patterns were collected on a Bruker D8 Advance powder diffractometer using a Ni-filtered Cu/K$\alpha$ radiation source at 40 kV and 20 mA, from 5 to 80° with a scan rate of 4° min$^{-1}$. The CHN elemental analysis was performed on an elemental analyzer Vario EL cube. The amount of leached molybdenum species in the filtrate was measured using a Jarrell-Ash 1100 ICP-AES spectrometer.

### 2.2 Preparation of catalysts

**Synthesis of $MoO_2(acac)_2$.** Molybdenyl acetylacetonate $MoO_2(acac)_2$ was prepared according to previous literature.[27] $(NH_4)_6MoO_{24}\cdot 4H_2O$ (30.0 g) was dissolved in $H_2O$ (100 mL) and acetylacetone (40 mL) was added. The pH of the solution was adjusted to 3.5 using 10% $HNO_3$ with the appearance of precipitated solids. Upon completion, the formed yellow precipitate $MoO_2(acac)_2$ (28.0 g, 51% yield) was filtered and washed with $H_2O$, ethanol, and ether, respectively, followed by drying in a vacuum.

**Synthesis of the oxo-molybdenum Schiff base (SB).** Oxo-molybdenum Schiff base complex SB-Mo was prepared according to previous literature.[22,23,28] To a stirred solution of 4-aminobenzoic acid (6.85 g, 0.05 mol) in ethanol (150 mL) was added salicylaldehyde (6.10 g, 0.05 mol), and the resulting mixture was stirred at room temperature for 30 min. The precipitated yellow Schiff base was separated from the reaction mixture by filtration and recrystallized with methanol to afford SB. To a stirred solution of Schiff base SB (2.41 g, 0.01 mol) in dry acetonitrile (20 mL) was added the prepared $MoO_2(acac)_2$ (1.19 g, 5 mmol), and the resulting mixture was refluxed for 12 h under a nitrogen atmosphere. The precipitated brown solid oxo-molybdenum Schiff base SB-Mo was filtered off and washed thoroughly by acetonitrile and diethyl ether, and dried under vacuum. $^1$H NMR (300 Hz, $CDCl_3$): $\delta$ (ppm) = 6.57 (m, 1H), 7.00 (m, 2H), 7.50 (d, 3H), 8.03 (d, 2H), 9.09 (s, 1H), 12.74 (s, 1H). Elemental analysis for SB-Mo (by the weight percentage): C 55.11%; H 3.14%; N 4.58%.

**Synthesis of octa(aminopropyl silsesquioxane) (POSS).** Octa(aminopropyl silsesquioxane) was prepared according to the previous literature.[7,29] Typically, deionized water (18 mL), propyl alcohol (8 mL), acetonitrile (2 mL), and tetraethyl ammonium hydroxide (0.4 mL) were added into a 500 mL flask to obtain a heterogeneous solution. $\gamma$-Aminopropyl triethoxysilane (44.0 g) was added into the solution, and the obtained mixture was heated to 50 °C with vigorous stirring. After reaction for 12 h, the formed white crystalline precipitate product POSS was filtered and washed with cold methanol three times, followed by drying in vacuum at 80 °C for 24 h.

**Synthesis of the POSS-bridged oxo-molybdenum Schiff base complex (POSS–SB-Mo).** The carboxylic acid groups (–COOH) in SB-Mo were converted to acid chloride (–COCl) using $SOCl_2$ according to the previous reports.[30,31] In a 100 ml round-bottom flask equipped with a magnetic stirring bar, $SOCl_2$ treated SB-Mo (0.64 g) was dissolved in ethanol (30 mL), and the solution was heated to 80 °C. Then, the aqueous solution of POSS (0.22 g) was added dropwise to the above mixture. The mixture was vigorously stirred at 80 °C for 12 h. Then, the green-colored precipitate was filtered and washed with $CH_3CN$ three times, and dried at 80 °C for 24 h to afford POSS–SB-Mo. Elemental analysis for POSS–SB-Mo (by the weight percentage): C 51.6%, N 7.11%, and H 4.09%, and the loading amount of Mo in the catalyst POSS–SB-Mo is calculated to be about 12.1%.

### 2.3 Catalytic test

Cyclooctene (1 mmol), $CHCl_3$ (5 mL), aqueous 65% TBHP (2 mmol), and POSS–SB-Mo (0.048 mmol) were added to a 25 mL flask. The resulting mixture was heated at 70 °C for 30 min. After completion of the reaction, the reaction mixture was analyzed using a gas chromatograph (GC, SP-6890A) equipped with a FID detector and a capillary column (SE-54 30 m × 0.32 mm × 0.25 μm). The catalyst was recovered by filtration and washed with ethanol, then dried in vacuum to obtain the recovered catalyst, and finally reused in the next run without addition of any fresh catalyst.

## 3. Results and discussion

### 3.1 Catalyst characterization

The synthetic functionalization route for POSS-bridged oxo-molybdenum Schiff base complex POSS–SB-Mo is shown in Fig. 1. Aminopropyl-POSS was synthesized according to a procedure reported in the literature.[29] The required oxo-molybdenum Schiff base was readily prepared by the two-step sequence involving condensation of salicylaldehyde

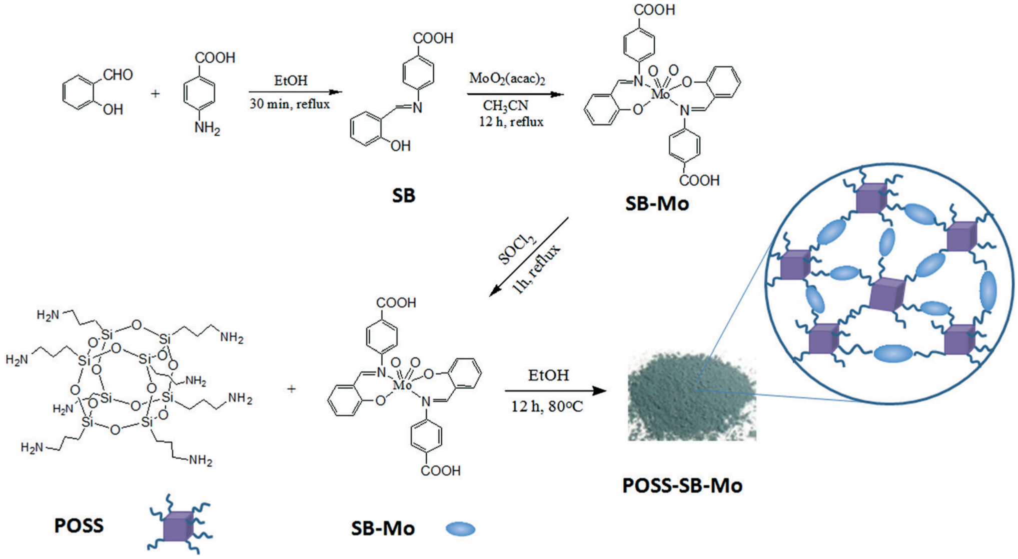

Fig. 1 Synthetic pathway for the POSS-bridged oxo-molybdenum Schiff base complex.

with 4-aminobenzoic acid to give Schiff base SB followed by its reaction with molybdenyl acetylacetonate $MoO_2(acac)_2$ in acetonitrile to yield oxo-molybdenum Schiff base SB-Mo in nearly quantitative yield. POSS–SB-Mo was then prepared as a green solid by reacting POSS with $SOCl_2$ treated SB-Mo in ethanol solvent at 80 °C for 12 h. Preparation of the POSS–SB-Mo catalyst and the intermediate steps were examined and monitored by $^1H$ NMR, XRD, FT-IR, SEM, and TGA. The resulting solid catalyst is insoluble in almost all the commonly used solvents, like ethanol, acetonitrile, chloroform, THF, DMF, *etc.* Thus the catalyst synthesized herein is favorable for heterogeneous catalysis.

The XRD patterns of both POSS and POSS–SB-Mo are shown in Fig. 2. POSS displayed well resolved identical peaks at 8° and 20° for the rhombohedral unit cell structure of the POSS inorganic segment (Fig. 2, curve a). However, the XRD pattern for POSS–SB-Mo indicates that the developed catalytic material is almost amorphous in nature, which is revealed by very weak and broad diffraction peaks as shown in Fig. 2, curve b.

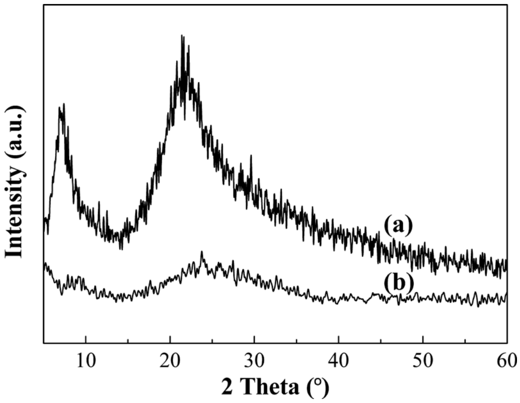

Fig. 2 XRD patterns of (a) POSS and (b) POSS–SB-Mo.

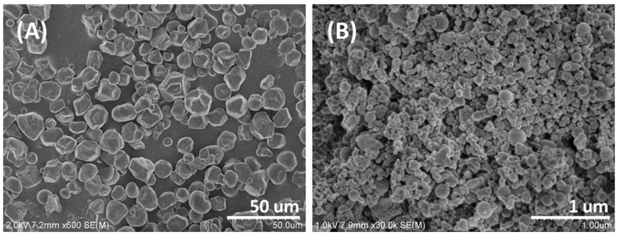

Fig. 3 SEM images of (A) SB-Mo and (B) POSS–SB-Mo.

Fig. 3 shows the SEM images of SB-Mo and POSS–SB-Mo. The oxo-molybdenum Schiff base is composed of irregular spherical particles with a size in micrometers (diameter: 10–30 μm, Fig. 3A). However, the particle size drops significantly with a diameter of about 50–200 nm upon using aminopropyl-POSS reagent as the monomer to prepare POSS–SB-Mo (Fig. 3B). The smaller particles of POSS–SB-Mo should be attributed to the unique three dimensional structure of the POSS monomer that isolates each substituted oxo-molybdenum Schiff base group on the vertices of POSS, which prevents the aggregation of SB-Mo into large particles. The pore structure and the surface area for these catalysts were characterized by nitrogen sorption experiments at 77 K. The results show that the catalyst POSS–SB-Mo is almost nonporous with a BET surface area of 30 $m^2$ $g^{-1}$, while the BET surface areas of POSS and SB-Mo are lower than 5 $m^2$ $g^{-1}$.

The chemical nature of the POSS-bridged oxo-molybdenum Schiff base catalyst and its intermediate products was revealed by FTIR. As shown in Fig. 4, the IR spectra of SB-Mo (Fig. 4, curve a) showed bands at 1703 $cm^{-1}$ assigned to stretching vibrations of C=O groups, 1606 $cm^{-1}$ due to C=N of the Schiff base and the characteristic bands at 948 and 905 $cm^{-1}$ for the symmetric and asymmetric stretching modes of the *cis*-$MoO_2$ fragment. An intense and broad peak which appeared at 2800–3500 $cm^{-1}$ in the spectrum of SB-Mo is attributed to the stretching mode of the O–H band, revealing

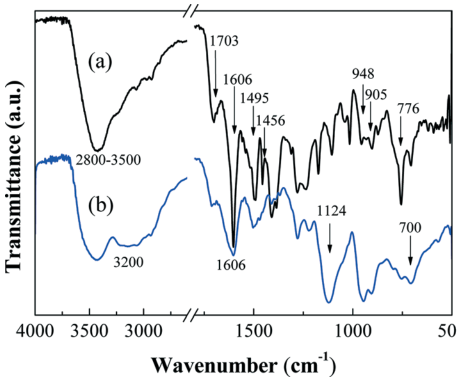

Fig. 4 FT-IR spectra of (a) SB-Mo and (b) POSS–SB-Mo.

the presence of COOH groups. Additionally, the bands around 1206 and 1060 cm$^{-1}$ are assigned to stretching vibrations of the aromatic ring, and the peak at 776 cm$^{-1}$ represents the *ortho*-substituted aromatic rings of the Schiff base. For the FTIR spectrum of POSS–SB-Mo (Fig. 4, curve b), these peaks appeared distinctively. Meanwhile, POSS–SB-Mo shows many new absorption peaks, in particular, peaks at 3200 and 700 cm$^{-1}$ reveal the presence of –NH groups of amide. The peak at 1124 cm$^{-1}$ illustrates the presence of Si–O–Si bonds. Furthermore, the C=N band at 1667 cm$^{-1}$ is broadened and the intensity of the bands corresponding to C=O and OH of the carboxylic group decreased. These vibrational signatures confirm the successful attachment of SB-Mo with POSS by covalent interactions.

The UV-vis profiles of POSS–SB-Mo and SB-Mo are compared in Fig. 5. POSS–SB-Mo showed an absorption band in the range of 600–800 nm that is assignable to the hydrogen bonds and intramolecular charge transfer from the amino groups –$NH_2$ in POSS to $MoO_2$ species;[32–34] however, the band was undetectable for SB-Mo, suggesting the reduction of $Mo^{6+}$ in POSS–SB-Mo by amino groups.

Fig. 6 illustrates TGA patterns for POSS–SB-Mo, POSS, and SB-Mo. The catalyst was found to be stable thermally up to *ca.* 250 °C, which is above the reaction conditions required for the liquid phase catalysis. The slight weight loss at the early heating stage below 250 °C results from the release of moisture and constitutional water. POSS shows about 45% weight loss between 250–700 °C, evidently owing to thermal decomposition of organic groups in POSS (Fig. 6, curve a), and SB-Mo shows a drastic weight loss of about 70% in the range 250–500 °C owing to the decomposition of the ligand moiety SB (Fig. 6, curve c). The TGA pattern for POSS–SB-Mo shows a weight loss of nearly 60% for the organic moiety (Fig. 6, curve b). Moreover, the elemental analysis for POSS–SB-Mo gave the data C: 51.6%, N: 7.11% and H: 4.09% (by weight percentage). From the results of TGA and elemental analysis, the molar ratio of POSS to SB-Mo is estimated to be 1:4 and the loading amount of Mo in POSS–SB-Mo is calculated to be 12.1%, demonstrating a high SB-Mo content in the catalyst.

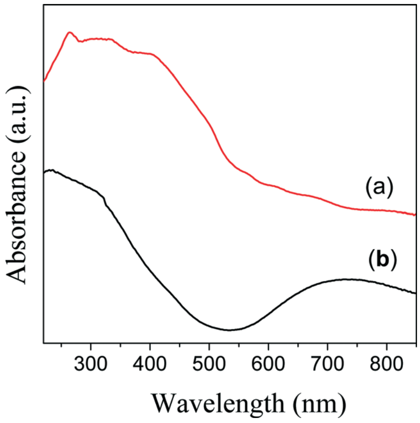

Fig. 5 UV-vis spectra of (a) SB-Mo and (b) POSS–SB-Mo.

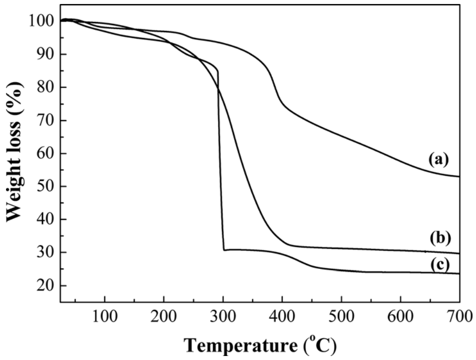

Fig. 6 TGA patterns of (a) POSS, (b) POSS–SB-Mo and (c) SB-Mo.

### 3.2 Catalytic activity in the epoxidation reaction

The catalytic efficiency of the prepared POSS-bridged oxomolybdenum Schiff base complex POSS–SB-Mo and comparison with its homogenous analogue were studied for epoxidation of cyclooctene using TBHP as the oxidant. The results of conversion and selectivity at different reaction times are given in Table 1. In the absence of the catalyst, the reaction did not proceed at all even after prolonged reaction times (Table 1, entry 1). The $MoO_2(acac)_2$ complex dissolved in the reaction medium to give a homogeneous system showed a high conversion of 95% with 98% selectivity at 0.5 h reaction time (Table 1, entry 2). A longer reaction time can increase the conversion of cyclooctene; however, this leads to a very low selectivity of 81%. SB-Mo exhibited higher catalytic activity than $MoO_2(acac)_2$. Good conversion of 99% with 100% selectivity could be obtained over a reaction time of 1 h (Table 1, entry 3), and the selectivity almost remained in a constant value with the increasing of the reaction time. However, SB-Mo was partly dissolved in the reaction medium during the epoxidation reaction, which leads to a low catalyst recovery ratio.

Interestingly, the POSS–SB-Mo catalyst showed the highest catalytic activity, where the catalytic epoxidation of cyclooctene was completed in about 30 min at a molar ratio of TBHP to cyclooctene of 2.0, giving a conversion of 99% and

**Table 1** Catalytic results of epoxidation of cyclooctene using TBHP by various catalysts[a]

| | | | Conversion/selectivity[b] at different reaction times (%) | | |
|---|---|---|---|---|---|
| Entry | Catalyst | Solubility | 0.5 h | 1 h | 1.5 h |
| 1[c] | — | — | n.d. | n.d. | n.d. |
| 2 | $MoO_2(acac)_2$ | Soluble | 95/98 | 99/93 | 100/81 |
| 3 | SB-Mo | Partly soluble | 82/100 | 99/100 | 100/100 |
| 4 | POSS–SB-Mo | Insoluble | 99/100 | 100/100 | 100/100 |

[a] Reaction conditions: catalyst (0.048 mmol), cyclooctene (1 mmol), $CHCl_3$ (5 mL), TBHP (2 mmol), 70 °C. [b] Selectivity for the epoxide product. Byproducts for entry 2 are 2-cycloocten-1-ol and 2-cycloocten-1-one. [c] The reactions are performed in the absence of the catalyst, and the conversions are too low to be determined (abbreviated as "n.d.").

selectivity of 100% (Table 1, entry 4). The conversion of 27% with 100% selectivity was obtained with an equimolar amount of TBHP to cyclooctene. It is worthwhile to notice that the suitable reaction time, 30 min, is much shorter than those for the previously reported catalysts, such as molybdenum dioxo complexes, oniumsilica-immobilized polyoxometalate, supported tungsten oxide, and metal–organic framework immobilized manganese(II) acetylacetonate complexes,[14,35–37] verifying the high efficiency of the present POSS-bridged oxo-molybdenum Schiff base catalyst POSS–SB-Mo. Moreover, facile recovery and recycling ability of POSS–SB-Mo make it a more superior catalyst. The results of the above control experiments imply that the featured three dimensional network framework of POSS–SB-Mo endows the catalyst with an insoluble nature in the reaction media, and that the POSS units in the complex POSS–SB-Mo play an essential role in improving the overall activity.

Heterogeneous catalysts generally exhibit much lower activities than homogeneous catalysts because the degree of exposure of the catalytically active sites to reactants is much lower over homogeneous catalysts.[38,39] However, the heterogeneous catalyst POSS–SB-Mo exhibited a much higher activity than its homogenous analogues SB-Mo and $MoO_2(acac)_2$ with the same number of active sites. It is noteworthy that the addition of POSS can improve the hydrophobic and oleophilic properties of the functional materials.[40,41] In the present study, the enhanced catalytic activity for this heterogeneous catalyst POSS–SB-Mo may be attributed to the hydrophobic property of the POSS monomer. To understand the role of POSS in catalysis, we carried out the contact angle (CA) tests. As shown in Fig. 7, when a droplet of cyclooctene or TBHP was brought in contact with the surface of POSS–SB-Mo, the CA was measured to be less than 5°. However, for a water droplet on the surface of POSS–SB-Mo, the CA was measured to be 105°. These phenomena indicate that POSS–SB-Mo is relatively hydrophobic and the reactants have good wettability on it. It is thus proposed that the hydrophobic three dimensional network structure of the catalyst POSS–SB-Mo should have supplied a unique microenvironment for the catalyst to involve the substrates alkene and TBHP during the epoxidation reaction, which allows Mo species in the bulk of the catalyst fully act as active centers.

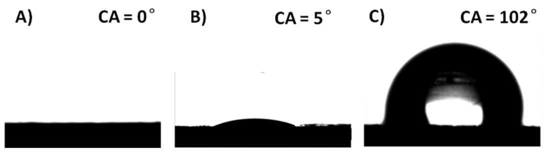

**Fig. 7** Contact angle for a droplet of (A) cyclooctene, (B) TBHP and (C) water on the surface of POSS–SB-Mo.

### 3.3 Solvent effects in the epoxidation reaction

The catalyst POSS–SB-Mo exhibits different performances in the epoxidation of cyclooctene with TBHP using various solvents. As shown in Fig. 8, in the solvents such as $CHCl_3$ and $CCl_4$ with no coordination ability to the metal center and low dielectric constant, high epoxidation conversions were obtained. In particular, for the $CHCl_3$ solvent, excellent conversion of 99% with 100% selectivity was observed in a short reaction time of only 0.5 h. The reactions in solvents such as $CH_2Cl_2$ and $CH_3COOC_2H_5$ were found to be slow, presumably due to the higher dielectric constants than that of $CHCl_3$. On the other hand, in the coordinated solvents, such as $CH_3CN$ with high coordinating ability to the metal center and high dielectric constant, very low epoxidation conversions were observed at every hour of the reaction time.

### 3.4 Epoxidation reactions with various substrates over POSS–SB-Mo and SB-Mo catalysts

We assessed the catalytic activity of POSS–SB-Mo and SB-Mo under the described reaction conditions, using a series of various types of aromatic and aliphatic alkenes. The results

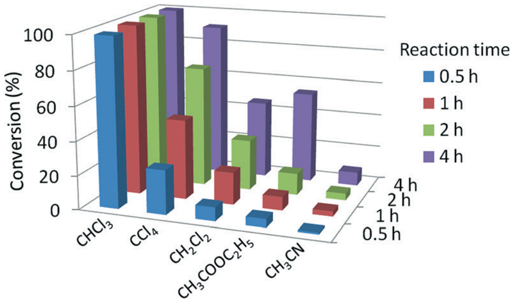

**Fig. 8** Catalytic performance of POSS–SB-Mo in epoxidation of cyclooctene with TBHP in different solvents. Reaction conditions: solvent (5 mL), cyclooctene (1 mmol), catalyst POSS–SB-Mo (0.048 mmol), TBHP (2 mmol), 70 °C.

**Table 2** Epoxidation of various substrates with TBHP over catalysts POSS–SB-Mo and SB-Mo[a]

| Entry | Substrate | Product | $t$ (h) | Con (%)<br>POSS–SB-Mo | Sel (%) | Con (%)<br>SB-Mo | Sel (%) |
|---|---|---|---|---|---|---|---|
| 1 | 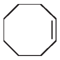 | 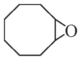 | 0.5 | 99 | 100 | 82 | 100 |
| 2 | 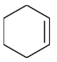 | 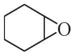 | 2 | 99 | 100 | 93 | 100 |
| 3 | 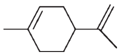 | 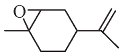 | 6 | 67 | 75 | 92 | 61 |
| 4 | 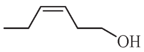 | 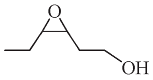 | 2 | 97 | 88 | 45 | 80 |
| 5 | 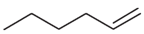 | 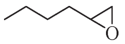 | 6 | 85 | 100 | 86 | 100 |
| 6 | 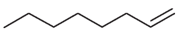 | 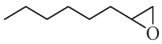 | 6 | 35 | 100 | 34 | 84 |
| 7 | 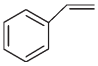 | 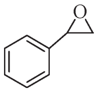 | 6 | 30 | 83 | 11 | 48 |
| 8 | 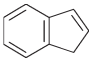 | 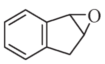 | 8 | 18 | 55 | 17 | 53 |

[a] Reaction conditions: solvent ($CHCl_3$, 5 mL), alkene (1 mmol), catalyst (0.048 mmol), TBHP (2 mmol), 70 °C.

are summarized in Table 2. It can be seen that the heterogeneous catalyst POSS–SB-Mo gave good to excellent conversions for the epoxidation of a range of alkenes and, encouragingly, in the majority of cases outperformed homogeneous SB-Mo. These results further suggest a catalytically promotional role of POSS for the epoxidation reaction. Moreover, as well known, higher electron donation ability of the olefin double bond is expected to show greater epoxidation reactivity. Therefore, cyclooctene, cyclohexene, and limonene with inner double bonds exhibit more activities in comparison with 1-hexene and 1-octene which contain terminal double bonds. Styrene and indene afforded very low conversions and selectivities mostly due to the presence of more electron withdrawing groups connected to the double bond.

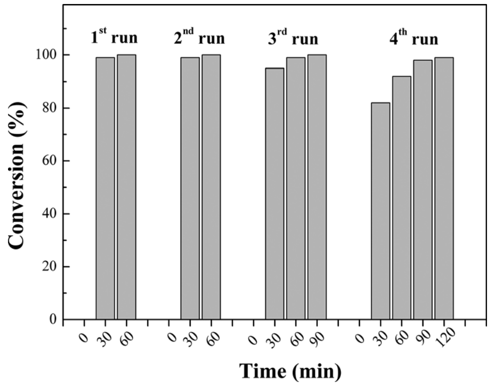

**Fig. 9** Catalyst recycling in epoxidation of cyclooctene with TBHP over POSS–SB-Mo.

### 3.5 Catalyst reusability

Further experiments were conducted to examine the recyclability and reusability of the POSS–SB-Mo in the epoxidation of alkenes using cyclooctene as a model substrate. At the end of the reaction, the catalyst recovered by simple filtration was washed with ethanol, dried and reused for the next run without adding any fresh catalyst. Fig. 9 shows the catalytic recycling properties for POSS–SB-Mo, suggesting quite a steady reusability for this complex catalyst without observing significant loss of conversion. In each run, only the corresponding epoxide was detected and no other ring-opening byproducts were found. In addition, the profiles of IR spectra for the recovered catalyst (Fig. 10) were in good agreement with that of the fresh one, demonstrating a very durable catalyst structure.

In order to test the possible catalysis of the slightly leached metal species in the reaction solution from the catalyst, an additional experiment was carried out. Initially, the mixture of the catalyst and TBHP in $CHCl_3$ was stirred at 70 °C for 20 min. The catalyst was then removed and the reaction proceeded for another 40 min with the homogeneous filtrate. It can be seen in Fig. 11 that no oxidation occurred. Furthermore, the result of ICP-AES elemental analysis for the reacted filtrate shows that less than 0.5 wt.% Mo in the catalyst leached into the reaction media. The above results strongly indicate the heterogeneous nature of the present catalyst POSS–SB-Mo for the epoxidation reaction. The slight decrease of the activity in the fourth run is mostly due to the weight loss in the operation for recovering the catalyst.

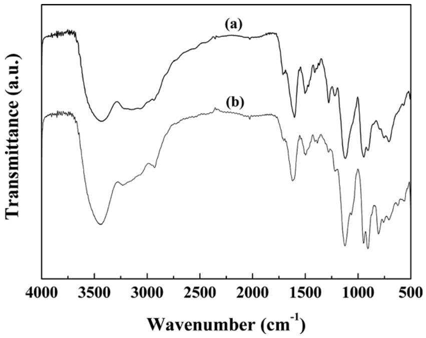

**Fig. 10** FT-IR spectra of (a) fresh POSS–SB-Mo and (b) reused POSS–SB-Mo.

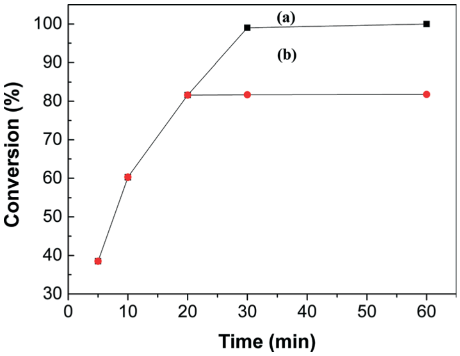

**Fig. 11** (a) Kinetic profile of epoxidation of cyclooctene with TBHP and (b) leaching experiment of POSS–SB-Mo (continuing the reaction after removing the catalyst after 20 min). Reaction conditions are analogous to Table 1.

## 4. Conclusions

In summary, we have demonstrated the successful application of aminopropyl-POSS as a building block for immobilizing the oxo-molybdenum Schiff base *via* covalent attachment. The prepared POSS-bridged oxo-molybdenum Schiff base complex POSS–SB-Mo was found to be a highly efficient catalyst for epoxidation of alkenes using aqueous TBHP as the oxidant. The catalyst was recovered easily and reused for four runs without observing significant loss in catalytic activity. The overall superior catalytic activity, high selectivity and excellent recyclability of POSS–SB-Mo as a heterogeneous catalyst could be attributed to its excellent structural stability and unique hydrophobic properties, which allow for a rapid and easy diffusion of the reactants into the reactive Mo centers.

## Acknowledgements

The authors thank the National Natural Science Foundation of China (No. 21206052), the Opening Foundation of the State Key Laboratory of Materials-Oriented Chemical Engineering (No. KL13-09), and MOE & SAFEA for the 111 Project (No. B13025).

## Notes and references

1 F. J. Feher, D. A. Newman and J. F. Walzer, *J. Am. Chem. Soc.*, 1989, **111**, 1741.
2 J. F. Brownand and L. H. Vogt, *J. Am. Chem. Soc.*, 1965, **87**, 4313.
3 H. Lin, J. Ou, Z. Zhang, J. Dong and H. Zou, *Chem. Commun.*, 2013, **49**, 231.
4 T. Nakanishi, T. Norisuye, H. Sato, T. Takemori, Q. Tran-Cong-Miyata, T. Sugimoto and S. Nomura, *Macromolecules*, 2007, **40**, 4165.
5 K. Tanaka and Y. Chujo, *J. Mater. Chem.*, 2012, **22**, 1733.
6 M. Seino, W. Wang, J. E. Lofgreen, D. P. Puzzo, T. Manabe and G. A. Ozin, *J. Am. Chem. Soc.*, 2011, **133**, 18082.
7 F. Wang, X. Lu and C. He, *J. Mater. Chem.*, 2011, **21**, 2775.
8 K. Tanaka, F. Ishiguro and Y. Chujo, *J. Am. Chem. Soc.*, 2010, **132**, 17649.
9 C. McCusker, J. B. Carroll and V. M. Rotello, *Chem. Commun.*, 2005, 996.
10 T. Ceyhan, A. Altındal, A. R. Ozkaya, B. Salih and O. Bekaroglu, *Dalton Trans.*, 2009, 10318.
11 Y. Chu, C. Cheng, Y. Chen, Y. Yen and F. Chang, *J. Mater. Chem.*, 2012, **22**, 9285.
12 S. Sakugawa, K. Wada and M. Inoue, *J. Catal.*, 2010, **275**, 280.
13 A. Kajetanowicz, J. Czaban, G. R. Krishnan, M. Malinska, K. Wozniak, H. Siddique, L. G. Peeva, A. G. Livingston and K. Grela, *ChemSusChem*, 2013, **6**, 182.
14 K. Kamata, K. Yonehara, Y. Sumida, K. Hirata, S. Nojima and N. Mizuno, *Angew. Chem., Int. Ed.*, 2011, **50**, 12062.
15 M. Herbert, E. Alvarez, D. J. Cole-Hamilton, F. Montilla and A. Galindo, *Chem. Commun.*, 2010, **46**, 5933.
16 S. P. Maradur, C. Jo, D. Choi, K. Kim and R. Ryoo, *ChemCatChem*, 2011, **3**, 1435.
17 Y. Leng, J. Wang, D. Zhu, M. Zhang, P. Zhao, Z. Long and J. Huang, *Green Chem.*, 2011, **13**, 1636.
18 K. C. Gupta and A. K. Sutar, *Coord. Chem. Rev.*, 2008, **252**, 1420.
19 P. G. Cozzi, *Chem. Soc. Rev.*, 2004, **33**, 410.
20 C. Che and J. Huang, *Coord. Chem. Rev.*, 2003, **242**, 97.
21 K. C. Gupta, A. K. Sutar and C. Lin, *Coord. Chem. Rev.*, 2009, **253**, 1926.
22 S. Jain and O. Reiser, *ChemSusChem*, 2008, **1**, 534.
23 S. L. Jain and B. Sain, *Adv. Synth. Catal.*, 2008, **350**, 1479.
24 H. P. Mungse, S. Verma, N. Kumar, B. Sain and O. P. Khatri, *J. Mater. Chem.*, 2012, **22**, 5427.
25 S. Verma, M. Nandi, A. Modak, S. L. Jain and A. Bhaumik, *Adv. Synth. Catal.*, 2011, **353**, 1897.
26 S. Sharma, S. Sinha and S. Chand, *Ind. Eng. Chem. Res.*, 2012, **51**, 8806.
27 G. J. Chen, J. W. Mcdonald and W. E. Newton, *Inorg. Chem.*, 1976, **15**, 2612.
28 S. J. Xia, F. X. Liu, Z. M. Ni, W. Shi, J. L. Xue and P. P. Qian, *Appl. Catal., B*, 2014, **144**, 570.
29 Z. Zhang, G. Liang and T. Lu, *J. Appl. Polym. Sci.*, 2007, **103**, 2608.
30 M. Moghadama, S. Tangestaninejad, V. Mirkhani, I. Mohammadpoor-Baltork and N. S. Mirbagheri, *Appl. Organomet. Chem.*, 2010, **24**, 708.

31 M. Moghadama, I. Mohammadpoor-Baltork, S. Tangestaninejad, V. Mirkhani, H. Kargar and N. Zeini-Isfahani, *Polyhedron*, 2009, **28**, 3816.

32 T. Yamase, *Chem. Rev.*, 1998, **98**, 307.

33 Q. L. Chen, H. B. Chen, Z. X. Cao and Z. H. Zhou, *Dalton Trans.*, 2013, **42**, 1627.

34 Y. Wu, J. Zheng, L. Xu, Z. Wang and D. Wen, *J. Electroanal. Chem.*, 2006, **589**, 232.

35 M. E. Judmaier, C. Holzer, M. Volpe and N. C. Mösch-Zanetti, *Inorg. Chem.*, 2012, **51**, 9956.

36 T. Kovalchuk, H. Sfihi, V. Zaitsev and J. Fraissard, *J. Catal.*, 2007, **249**, 1.

37 S. Bhattacharjee, D. Yang and W. Ahn, *Chem. Commun.*, 2011, **47**, 3637.

38 M. J. Climent, A. Corma and S. Iborra, *Chem. Rev.*, 2011, **111**, 1072.

39 V. K. Dioumaev and R. M. Bullock, *Nature*, 2003, **424**, 530.

40 L. Valentini, S. B. Bon, O. Monticelli and J. M. Kenny, *J. Mater. Chem.*, 2012, **22**, 6213.

41 W. Zhang and A. H. E. Müller, *Prog. Polym. Sci.*, 2013, **38**, 1121.